Absorption effects in the determination of anomalous scattering factors using x-ray refraction through a prism

W. K. Warburton
Institute of Physics, University of Southern California, 4676 Admiralty Way, Suite No. 932, Marina del Ray, California 90292

K. F. Ludwig, Jr.
Department of Applied Physics, Stanford University, Stanford, California 94305
(Received 31 October 1985)

X-ray refraction through a prism was recently revived as a technique for measuring the anomalous x-ray scattering factor f', but deviations between theory and experiment were seen which were accentuated above absorption edges. We show these to arise from absorption effects on the angle of refraction and derive an expression demonstrating that they can increase dramatically as the angle of incidence approaches the critical angle. This refinement markedly improves agreement between theory and experiment. Further, we derive an expression for the profile of the refracted x-ray beam, finding a Cauchy distribution (Lorentzian) and suggesting thereby a possible means to obtain

I. INTRODUCTION

A recent paper by Fontaine, Warburton, and Ludwig[1] (FWL) showed that the refraction of x rays through the corner of a GaAs prism could be employed effectively to measure the real dispersion correction f' to the x-ray atomic scattering factor f. Their error analysis suggested that the technique could be both sufficiently accurate and easy to use to become a more generally applicable method for obtaining accurate f' values for use in anomalous scattering experiments. In practice, however, an observation was made which FWL were unable to entirely explain. This was that, while there was good agreement below the Ga edge between the prism f' values and f' values computed by a Kramers-Kronig transformation of f'' data from an extended x-ray absorption fine structure (EXAFS) type of experiment[2] (hereafter denoted as KK f' values), a significant deviation of about $0.5e^-$ was found above the Ga edge. Near the As edge this deviation was more extreme, being $1.9e^-$ below the As edge and $2.7e^-$ above the edge. In both cases the prism values were more negative and the deviation increased in crossing the absorption edge. Theoretical estimates of f' made using the technique of Cromer and Liberman[3] showed essentially similar results.

Since the only experimental parameter changed in making the measurement across the edge was the input photon energy and since several points across the edge were taken disjunctively, we have concluded that the FWL analysis was insufficiently accurate in its treatment of the influence of absorption, and hence of the imaginary dispersion correction f'', on the angle of refraction. Because recent work on x-ray reflection from multilayers[4] has shown that classical optical theory works very well in the x-ray regime, provided that appropriate values of the optical constants are employed, we applied this method to the present problem. This treatment produces a concise relationship between the angle of refraction and f'' and shows that the corrections involved can become quite large as the angle of incidence approaches the critical angle θ_c for total external reflection. Including these correction terms, the agreement between the prism and KK f' values is improved, and a significant fraction of the deviation differences across the two absorption edges is removed, particularly at the As edge. We further derive an expression for the refracted beam profile, showing its dependence on the f' and f'' values and so suggesting an alternate technique for their determination.

II. THEORY

A. Propagation through the prism

The physical situation is as shown in Fig. 1. An incident plane wave falls on the prism's top surface at glancing angle θ_i. Entering the prism, it is refracted at angle θ', measured to the top surface. Leaving the prism, it is refracted again, emerging with angle θ'' to the top

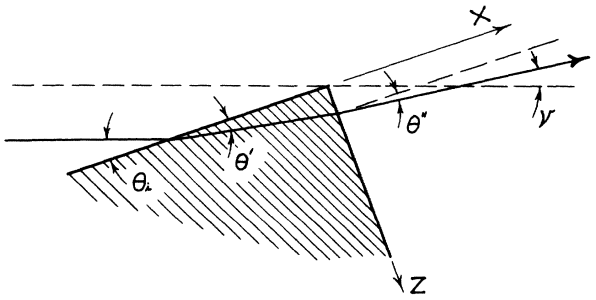

FIG. 1. Schematic of the x-ray experiment. The beam impinges on the prime at angle θ_i, is refracted at complex angle θ', and departs the prism at complex angle θ''. The refracted beam is measured externally at angle ν.

surface, which is parallel to the face normal, and making the experimentally measurable angle ν (unfortunately called β by FWL. β should be reserved for the imaginary part of the index of refraction) to the input beam of x rays. The refractive index of the outside air (vacuum) is unity, that of the material is $\hat{n}=1-\alpha-i\beta$, a complex number, where α and β are typically very small compared to unity, usually of order 10^{-4} or less. Our treatment will follow Stratton's,[5] although that of Born and Wolf[6] is similar.

Applying Snell's law at the two interfaces, we have

$$\cos\theta_i=\hat{n}\cos\theta' , \tag{1}$$

$$\hat{n}\sin\theta'=\sin\theta'' . \tag{2}$$

Because $\cos\theta_i$ is real and $\hat{n}$ complex, θ' must also be complex, showing that in the medium the wave is inhomogeneous, meaning that its planes of constant amplitude and constant phase are nonparallel. We can now solve formally for $\sin\theta''$ using the relationship $1=\cos^2\theta'+\sin^2\theta'$. Thus

$$\sin\theta''=(\hat{n}^2-\cos^2\theta_i)^{1/2}$$

and

$$\cos\theta''=(1-\hat{n}^2+\cos^2\theta_i)^{1/2} , \tag{3}$$

showing that $\sin\theta''$, and thus θ'', are clearly complex. This implies that the wave departing the prism is inhomogeneous as well, even though it is propagating in a medium with a real index of refraction. Figure 2 demonstrates the meaning of this conclusion. Two rays, A-A'' and B-B'', pass through the prism. Clearly ray B-B'' has a longer path length in the absorbing medium and so must have a smaller amplitude when it emerges. Since the final medium is nonabsorptive, neither ray can have a further change in amplitude in its direction of propagation. Thus amplitude decreases from A'' to B'', showing that the emerging wave is indeed inhomogeneous with its planes of constant amplitude *orthogonal* to its planes of constant phase. We will demonstrate this mathematically shortly.

Next, to obtain explicit complex representations for both $\cos\theta''$ and $\sin\theta''$, we will use the small angle expansion $\cos\theta_i=1-\theta_i^2/2$, dropping α^2 and β^2 terms in $\hat{n}^2$. Thus

$$\cos\theta''=1+\alpha-\theta_i^2/2+i\beta \tag{4}$$

and

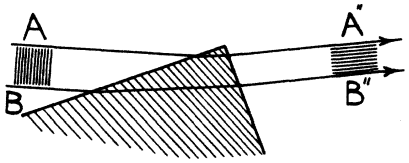

FIG. 2. Incoming x-ray beam with its planes of constant intensity perpendicular to the direction of propagation. In the outgoing beam they are parallel as a result of absorption inside the prism.

$$\sin\theta''=(\theta_i^2-2\alpha-2i\beta)^{1/2}=(\theta_d^2-2i\beta)^{1/2} , \tag{5}$$

where we have defined $\theta_d^2=\theta_i^2-2\alpha$, which is the *difference* between the squares of the angle of incidence and the critical angle for total external reflection, $\theta_c^2=2\alpha$.

Since $\sin\theta''$ is complex, we may set it equal to $\phi+i\gamma$ and solve for ϕ and γ by equating real and imaginary parts of

$$\phi^2+2i\phi\gamma-\gamma^2=\theta_d^2-2i\beta , \tag{6}$$

giving

$$\phi^2-\gamma^2=\theta_d^2 \quad \text{and} \quad \phi\gamma=-\beta . \tag{7}$$

These are solved by substituting for γ and choosing the sign of the root for ϕ such that $\phi=\theta_d$ when $\beta=0$ and the sign of the root for γ such that $\phi\gamma=-\beta$ as per Eq. (7). Thus,

$$\phi=\theta_d\left[\frac{(1+4\beta^2/\theta_d^4)^{1/2}+1}{2}\right]^{1/2}$$

and

$$\gamma=-\theta_d\left[\frac{(1+4\beta^2/\theta_d^4)^{1/2}-1}{2}\right]^{1/2} . \tag{8}$$

Possessing these expressions for $\cos\theta''$ and $\sin\theta''$, we can finally write an expression for the wave fields associated with our inhomogeneous exit beam. This beam is described by $\exp[i(\mathbf{k}''\cdot\mathbf{r}-\omega t)]$, and the spatial term in the exponent is

$$i\mathbf{k}''\cdot\mathbf{r}=i\frac{\omega}{c}(x\cos\theta''+z\sin\theta'')$$

$$=-\frac{\omega}{c}\{(x\beta+z\gamma)+i[x(1+\alpha-\theta_i^2/2)+z\phi]\} , \tag{9}$$

where we have used the x-z coordinate system shown in Fig. 1. Planes of constant amplitude are given by the real part of Eq. (9) (i.e., $x\beta+z\gamma=$const) and planes of constant phase are given by the imaginary part $xp+z\phi=$const, defining $p=1+\alpha-\theta_i^2=1-\theta_d^2/2$ for convenience. Our solutions for the planes are simplified by noting that $p\gg\phi$ and $\gamma\gg\beta$.

The direction of propagation of the exit beam is found as the normal to a typical plane of equal phase: $xp+z\phi=1$. Shown in Fig. 3, this normal forms angle θ_0 to the top of the prism, i.e., $z=0$. Notice that θ_0 is the

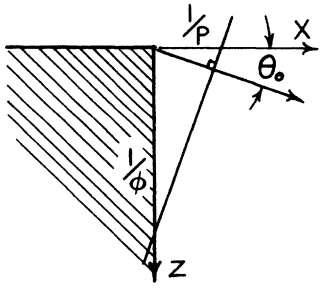

FIG. 3. Planes of equal phase in the emerging x-ray beam, by definition perpendicular to the direction of propagation at angle θ_0, which intercept the x and z axes as shown.

real angle of emission and must be distinguished from θ'', the *complex* angle of emission, which is a mathematical construct. The plane's x and z intercepts are $1/p$ and $1/\phi$, respectively, found by setting z and x equal to 0 in its defining equation. Since $p \gg \phi$, we have

$$\theta_0 \cong \tan\theta_0 = \phi/p \cong \phi \ , \tag{10}$$

since the difference terms between p and unity are $O(\alpha)$ and may be dropped. Thus we obtain the refined equation equivalent to Eq. (2) of FWL:

$$\theta_0^2 = \theta_d^2 \left[\frac{1+(1+4\beta^2/\theta_d^4)^{1/2}}{2} \right] , \tag{11}$$

where θ_0 is the angle of propagation of the beam coming out of the prism.

We note that planes of constant intensity are found similarly by reference to the plane $x\beta + z\gamma = 1$, whose normal is at angle ξ to the $x=0$ plane. The x and z intercepts are $1/\beta$ and $1/\gamma$, respectively, so that

$$\xi \cong \tan\xi = \beta/\gamma \ , \tag{12}$$

and we may substitute for β from Eq. (7) to obtain

$$\xi = -\phi\gamma/\gamma = -\phi = -\theta_0 \ . \tag{13}$$

This demonstrates that the planes of constant intensity are indeed orthogonal to the planes of constant phase, in agreement with our intuitive picture. We can therefore further conclude that the intensity profile of the emerging radiation depends only on its projected path through the prism corner.

B. Propagation beyond the prism

We will now consider the propagation of the x-ray beam once it departs the prism corner. This radiation source, as described by Eq. (9), is quite unusual, being both nonuniform (decays exponentially in the z direction) and spatially small. With typical estimates of α and β, most of the observed radiation emerges from the upper 1000 Å or less. Interference effects will therefore be important in determining the shape and possibly the direction of the observed beam.

This problem is one of relating electromagnetic fields to their sources and is readily approached by the Kirchhoff method of integration of the field equation. As Fig. 4 shows, we place the prism in the left half-plane and consider propagation in the right half-plane, where we must solve the homogeneous wave equation in an isotropic, source-free region of zero conductivity. Under these conditions, if ψ is a scalar potential or field vector component, then its value at point P and time t is given by[7]

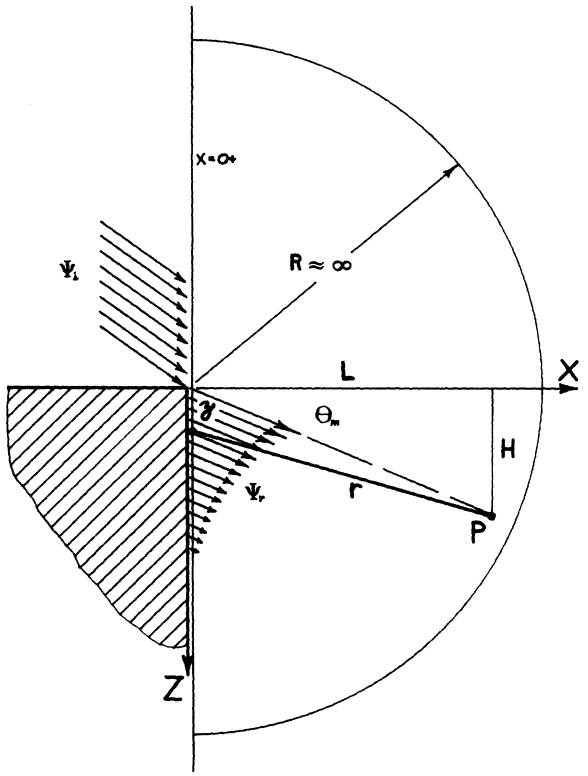

FIG. 4. Schematic of the integration scheme for computing the field $\psi(P,t)$ at remote location P, whose x and z coordinates are L and H and which makes angle θ_m to the x axis. A surface integral is taken over the plane at $0+$ and over a hemisphere whose radius R approaches infinity. Shown is the contribution via a typical surface element dz at position z of the refracted wave field ψ_r. The incident wave field ψ_i is ignored.

$$\psi(P,t) = \frac{1}{4\pi} \int_s \left\{ \frac{1}{r} \left[\frac{\partial\psi}{\partial n} \right] - \frac{\partial}{\partial n} \left[\frac{1}{r} \right] [\psi] + \frac{1}{vr} \frac{\partial r}{\partial n} \left[\frac{\partial\psi}{\partial t} \right] \right\} dS \ . \tag{14}$$

The terms in square brackets [ ] are *retarded* (i.e., functions of $t - r/v$), v is the velocity of propagation (here equal to c), and r is the vector from dS to the point P, whose coordinants are L and H, as indicated in Fig. 4. The integral may be taken over any surface enclosing the point P. Knowing the field emerging from the prism at $x=0$, we choose S to be bounded by a plane at $0+$ (infinitesimally close to $x=0$) and by a half-sphere of radius R centered on the prism. Letting R become infinite, the fields and integral on this surface go to zero, leaving only an integral on the $0+$ plane.

Two fields penetrate the $0+$ plane: the incident beam ψ_i and the refracted beam ψ_r. Assuming that these beams are well separated in space, we neglect the former, setting the surface integral on $0+$ to zero for $z<0$. Thus, from Eq. (9) above, we may write

$$\psi|_{0+} = \exp\left[\frac{-\omega}{c} \left\{ (x\beta + z\gamma) - i \left[x \left[1 - \alpha - \frac{\theta_i^2}{2} \right] + z\phi \right] - ict \right\} \right]_{0+} \tag{15}$$

and

$$r=[L^2+(H-z)^2]^{1/2} . \tag{16}$$

The partial derivatives in Eq. (14) are then easily written and substituted to obtain

$$[\psi]_{0+}=\exp\left[\frac{\omega}{c}(-z\gamma+i[z\phi-ct+\{L^2+(H-z)^2\}^{1/2}])\right] , \tag{17a}$$

$$\left[\frac{\partial\psi}{\partial n}\right]_{0+}=\frac{\omega}{c}\left\{-\beta+i\left[1-\alpha-\frac{\theta_i^2}{2}\right]\right\}[\psi]_{0+} , \tag{17b}$$

$$\left[\frac{\partial\psi}{\partial t}\right]_{0+}=-i\omega[\psi]_{0+} , \tag{17c}$$

$$\psi(P,t)=\frac{1}{2\lambda}\int_0^\infty\frac{dz}{r}[\psi]_{0+}\left[\left\{-\beta+i\left[1-\alpha-\frac{\theta_i^2}{2}\right]\right\}\frac{\lambda L}{2\pi r^2}+\frac{iL}{r}\right] . \tag{18}$$

Before proceeding, several simplifying approximations are appropriate. First, $\lambda L/2\pi r^2$ is $O(10^{-10})$ and may be neglected compared to the remaining terms. Second, since H/L is $O(10^{-3})$ and $z\ll H$ over the range of appreciable $[\psi]_{0+}$ values, we have as a good approximation

$$L/R\cong 1-H^2/2L^2 . \tag{19}$$

So we have

$$\psi(P,t)=\frac{1}{2\lambda}\int_0^\infty\frac{dz}{r}[\psi]_{0+}\left[-\beta+i\left\{\left[1-\alpha-\frac{\theta_i^2}{2}\right]+\left[1-\frac{H^2}{2L^2}\right]\right\}\right] . \tag{20}$$

We can now neglect terms like α, $\theta_i^2/2$, and $H^2/2L^2$ compared to unity to get the relatively simple integral equation

$$\psi(P,t)=K\int_0^\infty\frac{dz}{r}[\psi]_{0+}, \quad \text{where } K=\frac{2i-\beta}{2\lambda} . \tag{21}$$

Next we expand r to second order in z to obtain $r=R_0-Hz/R_0+z^2/2R_0$, and then note that only the deviations of r from R_0 in the exponential will seriously influence the integral's value. Thus

$$\psi(P,t)=K'\int_0^\infty dz\exp\left\{\frac{\omega}{c}\left[-z\gamma+i\left[z\phi-\frac{Hz}{R_0}+\frac{z^2}{2R_0}\right]\right]\right\} , \tag{22}$$

where

$$K'=KR_0^{-1}\exp[i\omega(R_0/c-t)] .$$

If we consider the z^2 term in the exponential, we see that it is very small and that we can make a small angle expansion to first order:

$$\exp\left[\frac{i\pi z^2}{\lambda R_0}\right]\cong 1+i\frac{\pi z^2}{\lambda R_0} , \tag{23}$$

where we have replaced $\omega/2c$ by π/λ and H/R_0 by θ_m, the angle of measurement. Thus we finally obtain

$$\frac{\psi(P,t)}{K'(R_0,t)}=\int_0^\infty dz\exp\left[\frac{-\omega z}{c}[\gamma+i(\theta_m-\phi)]\right]+\frac{i\pi}{\lambda R_0}\int_0^\infty dz\,z^2\exp\left[\frac{-\omega z}{c}[\gamma+i(\theta_m-\phi)]\right] . \tag{24}$$

Both of these integrals are available in standard handbooks,[8] so we are able to write

$$\psi(P,t)=\frac{K'\lambda}{2\pi}\left[\frac{1}{\gamma+i(\theta_m-\phi)}\right]\left[1+\frac{i\lambda}{2\pi R_0}[\gamma+i(\theta_m-\phi)]^{-2}\right] . \tag{25}$$

The measured intensity is obtained by squaring $\psi(P,t)$, so we thus obtain as our description for the diffracted beam

$$I(\theta_m)=\frac{1}{(2\pi R_0)^2}\left[\frac{1}{\gamma^2+(\theta_m-\phi)^2}\right]\left[1+\frac{2\lambda(\theta_m-\phi)\lambda}{\pi R_0[\gamma^2+(\theta_m-\phi)^2]^2}\right] , \tag{26}$$

where smaller terms have been dropped and β has been neglected compared to unity in K'. The second bracketed term arises entirely from z^2 in the expansion for r in Eq. (20).

In broad terms, then, the diffracted beam is predicted to have a Cauchy distribution whose mode is ϕ, the direction of propagation of planes of equal phase of the emerging x-ray beam [see Eq. (10)], and whose FWHM is 2γ, the constant for the exponential decay versus depth of the emerging x-ray beam [see Eq. (9)]. For fixed R_0 and λ, the shape of this distribution is determined entirely by ϕ and γ, the real and imaginary parts of $\sin\theta''$, the x-ray beam's *complex* angle of emergence from the prism face. The Cauchy distribution $C(x)$, which is familiar to physicists as the Lorentzian, is peculiar[9] in that it does not possess a well-defined expected value [since the integral of $xC(x)$ behaves as $\log(x)$ as x goes to $+\infty$ and as $-\log(x)$ as x goes to $-\infty$], but is well behaved in other respects. The genesis of this Cauchy distribution lies explicitly in the decaying exponential nature of the emerging beam, as opposed, for example, to its small size. As a computational check, for example, we repeated our derivation with a *constant* source of width $1/\gamma$, and checked that $I(\theta_m)$ displayed the multilobed diffraction pattern typically observed from slits.

To test the validity of this treatment, we computed refracted beam shapes at the five energies near the Ga edge shown in Fig. 3 of FWL, using their reported f' and f'' values. We neglected the small bracketed correction term in Eq. (26) and set the overall scale at each energy by matching peak heights. In Figs. 5(a) and 5(b) these calculations are compared to curves of FWL. The general agreement is excellent, although a few small discrepancies remain. The most obvious is that the real data appear to sit on a small background which has not been included in the calculation. Less obvious, but harder to explain, is the observation that the computed curves are noticeably narrower than the real data for the two lower energies (about 25% narrower at 10345 eV). Approximately half of the discrepancy can be accounted for by convolving the curves with the diffractometer 25-μ exit slit of FWL. If the slit used by FWL was actually wider than reported (i.e., 50 μ) or slightly skewed, the computed and measured curves would come into essentially exact agreement.

Finally, we can estimate the amount by which the small correction term, introduced by z^2 into Eq. (26), skews the Cauchy distribution. In the absence of the shift, the distribution has a full width at half maximum (FWHM) defined by $\theta_m-\phi=\pm\gamma$. The FWHM is thus -2γ. We next ask how these points are moved as a result of the z^2 skewing. In doing so we can replace the correction term's Cauchy denominator, which we expect to be small, by its approximate value $2\gamma^2$. We thus require values of θ_m to solve

$$\frac{1}{2\gamma^2}=\frac{1}{\gamma^2+(\theta_m-\phi)^2}\left[1+\frac{\lambda}{2\pi R_0\gamma^2}\right]. \tag{27}$$

If we approximate $\theta_m-\phi=\pm\gamma+\gamma\delta$, expand in small δ, and drop second order terms, we find

$$\pm\delta=\frac{\lambda}{2\pi R_0\gamma^2}, \tag{28}$$

meaning that the two FWHM points are $\phi+\gamma+\gamma\delta$ and $\phi-\gamma+\gamma\delta$. Thus the peak center has essentially shifted (to *smaller* angles, since γ is negative) by

$$\Delta\theta_0=-\lambda/(2\pi R_0\,|\,\gamma\,|\,). \tag{29}$$

C. Solution for the anomalous scattering factor f'

Temporarily neglecting the small z^2 error term between the direction of our output beam and $\theta_0=\phi$, as represented by Eq. (29), we can now solve for the anomalous scattering factor f' in terms of our experimental parame-

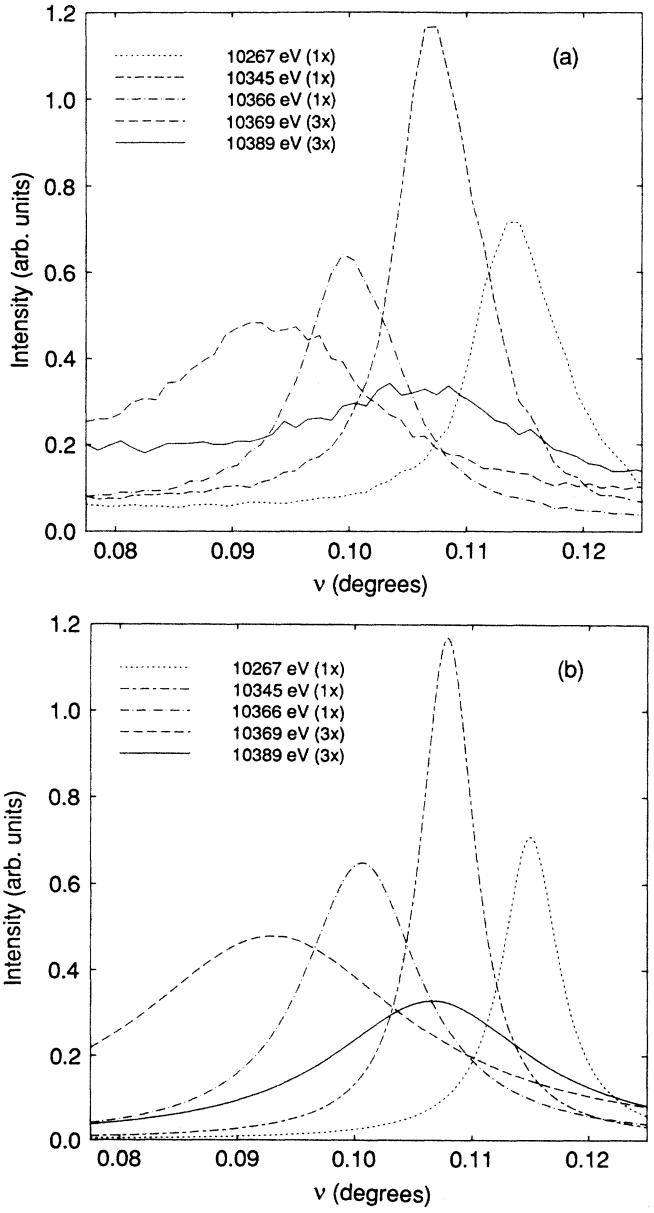

FIG. 5. Comparison between (a) five measured x-ray beam profiles (Fig. 3 of FWL, replotted) and (b) Cauchy profiles computed using the f' and f'' values of FWL at these energies.

ters, starting from Eq. (11). First, we recall that f' is part of the index of refraction term α, which is hidden in θ_d. Explicitly,

$$\theta_0^2=\left[\frac{\theta_i^2-2\alpha}{2}\right]\left\{1+\left[1+\frac{4\beta^2}{(\theta_i^2-2\alpha)^2}\right]^{1/2}\right\}, \tag{30}$$

or

$$\alpha=\tfrac{1}{2}[\theta_i^2-\theta_0^2+\beta^2/\theta_0^2]\ . \tag{31}$$

The relationships between the optical constants α and β and the anomalous scattering factors f' and f'' are, as shown by James:[10]

$$f'=C\alpha-Z_T \quad \text{and} \quad f''=C\beta\ , \tag{32}$$

where

$$C=(2\pi mc^2)/(N\lambda^2e^2)\ , \tag{33}$$

in which all the terms have their usual meanings, including N, the number of point groups (e.g., gallium atoms) per unit volume, and $Z_T=Z_{\mathrm{Ga}}+Z_{\mathrm{As}}$, the total number of electrons in the two atoms making up the point group. In this notation, of course, $f'=f'_{\mathrm{Ga}}+f'_{\mathrm{As}}$, the sum of the anomalous scattering factors of the atoms in the point group, and similarly with f''. Substitution of Eqs. (31) and (33) into (32) gives

$$f'=\frac{C}{2}(\theta_i^2-\theta_0^2)+\Delta f'_a-Z_T\ , \tag{34}$$

where

$$\Delta f'_a=\frac{(f'')^2}{2C\theta_0^2} \tag{35}$$

is the correction term introduced by absorption effects. In terms of the experimentally accessible angles θ_i and ν, this gives

$$f'=\frac{C}{2}(2\theta_i\nu-\nu^2)+\frac{(f'')^2}{2C(\theta_i-\nu)^2}-Z_T\ . \tag{36}$$

Repeating this analysis including the error term $\Delta\theta_0$ from Eq. (29) shows that the source shape interference effects contribute an additional term to Eq. (34), reducing the effective value of f' measured. This term, $\Delta f'_s$, is found from a first-order expansion of Eq. (31) as

$$\Delta f'_s=-C\lambda\phi/(2\pi R_0\,|\,\gamma\,|\,)\ , \tag{37}$$

where we have replaced θ_0 by the measured value ϕ.

III. DISCUSSION AND ANALYSIS

A. Features of the theory

Compared to the equation 2 of FWL, Eqs. (34) and (35) demonstrate the nature of the absorption-dependent correction term $\Delta f'_a$, which varies as the square of the absorption f'', and as the inverse square of θ_0. This latter term causes $\Delta f'_a$ to become large as the incident beam approaches the critical angle θ_c, since, to first order, θ_0^2 equals θ_d^2, the difference between θ_i^2 and $\theta_c^2=2\alpha$ [see Eq. (11)]. In the limit, as $\theta_i=\theta_c$, both higher-order corrections and the square-root term in Eq. (11) prevent $\Delta f'_a$ from diverging. In practice, $\Delta f'_a$ is usually less than 25% of f'.

The source shape correction term $\Delta f'_s$ is also interesting in that it becomes larger as the absorption term β (and f'') becomes smaller. For example, in the small f'' limit

$$\Delta f'_s=-\lambda(\theta_i^2-2\alpha)/(4\pi R_0 f'')\ , \tag{38}$$

showing that in our current material, GaAs, $\Delta f'_s$ will be largest just below the Ga absorption edge. While $\Delta f'_s$ will be small in the present problem, it can potentially become large when f'' is very small, as in low-Z materials, for example.

To illustrate these effects on the data of FWL, we present values of $\Delta f'_a$ and $\Delta f'_s$ above and below both the Ga and As edges. To clarify the comparison, the two points at each edge were chosen with equal deflection angles ν (β in Figs. 4 and 5 of FWL). The resultant values of f'', θ_i, θ_0, f'_a, and $\Delta f'_s$ are listed in the first half of Table I. We see immediately that $\Delta f'_a$ is much larger at the As edge than at the Ga edge both because the f'' values are larger there and because the As measurement was performed about three times closer to the critical an-

TABLE I. Values of correction terms to f' and sensitivities to error at four points above and below the Ga and As absorption edges in the measurements of FWL.

Quantity	Ga^-	Ga^+	As^-	As^+
E (eV)	10338	10400	11845	11875
f'' (e^-)	1.2	4.4	3.6	7.0
θ_i (deg)	0.298	same	0.223	same
$\theta_i-\theta_c$ (deg)	0.069	same	0.025	same
θ_0 (deg)	0.191	same	0.102	same
$\Delta f'_a$ (e^-)	0.009	0.124	0.222	0.84
$\Delta f'_s$ (e^-)	−0.021	−0.005	−0.002	−0.001
$\partial f'/\partial\theta_m$ (e^-/deg)	220	same	350	same
$\partial f'/\partial\nu$ (e^-/deg)	400	same	300	same
$\partial f'/\partial\theta_z$ (e^-/deg)	−520	same	−450	same
$\partial\Delta f'_a/\partial\theta_0$ (e^-/deg)	0.1	1.3	4.4	16.4

gle. The source shape correction, $\Delta f_s'$, is largest below the Ga edge, as predicted, but is always negligible compared to the magnitudes of f' being measured.

Also shown in Table I are estimates of the sensitivities of f' to various sorts of measurement error, as discussed in FWL. θ_z is the experimentally determined zero of angle. The last term is new, being the error in the correction term which results from uncertainties in the measurement of θ_0 and which is negligible in the present case. In fact, the direct errors in f' associated with uncertainties in θ_m, θ_z, and ν are two to three orders of magnitude larger and still constitute the source of the major uncertainty in f'.

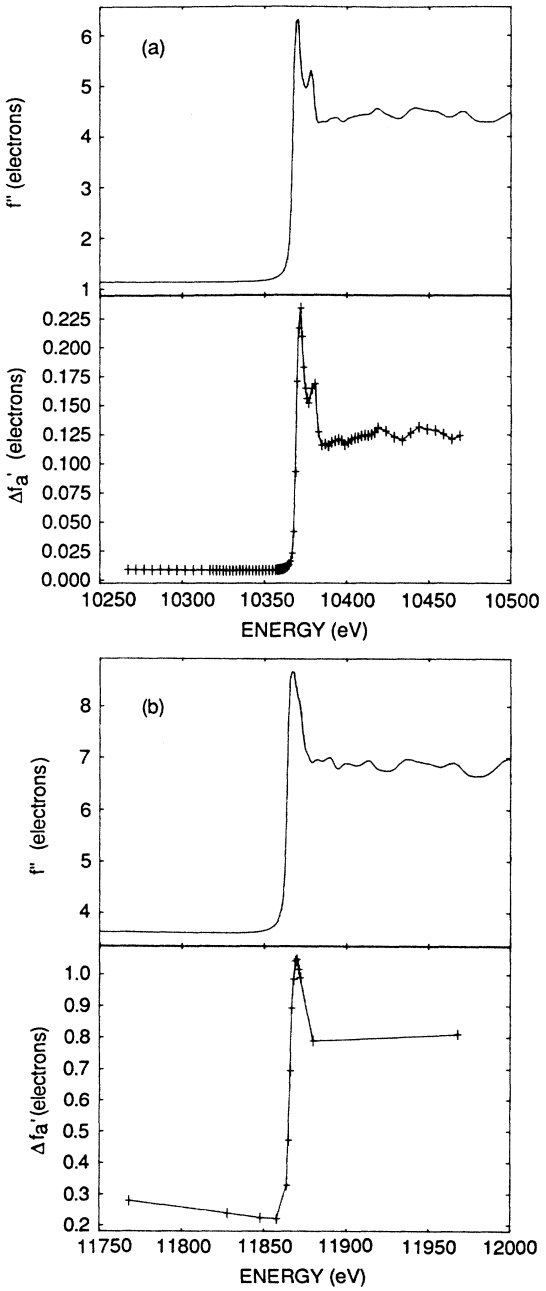

FIG. 6. Correction terms $\Delta f_a'$ and the f'' values from which they are derived at (a) the Ga edge and (b) the As edge.

B. Effect on the data curves

We shall now examine in detail the changes produced in the f' curves of FWL by the inclusion of the absorption term $\Delta f_a'$ from Eqs. (34) and (35). Figure 6(a) shows the anomalous scattering factor f'' near the Ga edge, as obtained by FWL from EXAFS data, and the computed correction term $\Delta f_a'$. The dependence of $\Delta f_a'$ on f'' squared is most clearly seen at the white line on the absorption edge. Figure 6(b) shows the corresponding data from the As edge, where the largest corrections are found, in accordance with the numerical example of Sec. III A. The maximum corrections found are over $1e^-$ and are clearly nontrivial in nature.

Figures 7(a) and 7(b) show the corrected f' curves, together with the uncorrected data and KK f' estimates of Figs. 6(a) and 6(b) of FWL. The changes produced at the Ga edge are in the right direction but only 25–30% of the magnitude required to bring the prism and KK f' values into good agreement. The changes at the As edge are much larger, but also insufficient to create agreement with the KK curves. The inequality between the

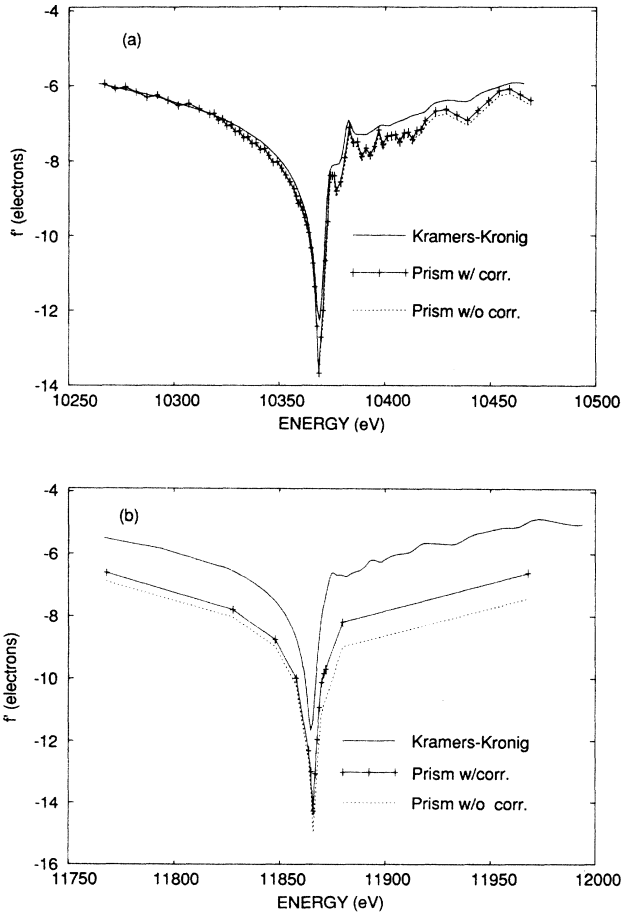

FIG. 7. f' values at (a) the Ga edge and (b) the As edge. The three curves shown are the KK f' values, f' values from the prism experiment of FWL, and these same values after correction by the $\Delta f_a'$ values of Fig. 6.

discrepancies above and below the As edge have been substantially reduced, however. As was noted in FWL, a *uniform* discrepancy between prism and KK results is readily explicable in terms of measurement errors in the fixed angles θ_i and θ_z, so the reduction of that inequality is a significant improvement. It is particularly interesting to note that, if the As data are shifted uniformly upward to superimpose the below-edge data with the KK data, then the above-edge differences are nearly identical for *both* As and Ga. This suggests that some further, absorption-dependent mechanism may be operating which still remains to be identified. The still sizable differences remaining at the white lines may arise from the same source but could also be due to monochromator energy resolution differences between the EXAFS data used to produce the KK f' values and the data of the experiment of FWL.

C. Experimental considerations for accurate f' values

In selecting θ_i for an experiment, the implications of Eqs. (34) and (35) must be carefully considered if accurate f' values are to be obtained. The choice will be decided by balancing two factors. First, since both θ_i and θ_0 have experimental uncertainties, the maximum accuracy in α, which varies as the difference of their *squares,* would normally be obtained when both are as small as possible. This situation would occur as θ_i approaches θ_c, the critical angle, and θ_0 goes to zero. Second, there is now also a second factor to be considered, $\Delta f_a'$, which varies *inversely* as θ_0^2 and becomes large in this case. Thus the value of θ_i which gives the minimum total error must depend upon the accuracy with which f'' is known or can be determined. A further consideration, of a practical nature, is that as θ_i becomes smaller, both a larger fraction of the prism surface and a smaller depth at the edge are sampled. Thus the requirements for surface and edge perfection increase as θ_i decreases, another argument against approaching θ_c too closely.

If accurate f'' values are known, from an EXAFS experiment or otherwise, then they can be used with Eq. (35) to obtain accurate f' values as well. If, however, f'' values are either unknown for the material composition of interest or are only available from either free-atom or theoretical curves which do not include edge related structure, then this procedure is less satisfactory. In particular, both near edge and EXAFS modulations will be superimposed, squared, on the data. In this situation, one approach might be to employ measured f' values in an iterative self-correction scheme, using KK transforms to generate succeeding f'' approximations for insertion into Eq. (35). The situation is much simpler if f' values are only required *below* an absorption edge (e.g., for application in anomalous scattering experiments). Here f'' is a smoothly varying function which can usually be computed with acceptable accuracy either from theory or tabulated absorption coefficients, thus allowing $\Delta f_a'$ to also be determined with acceptable accuracy, provided θ_0 is not too small. In many practical cases, then, we can expect to increase the accuracy of the f' determination without unduly increasing the effort of performing it.

D. Alternative approach to accurate f' values

A different approach to obtaining accurate f' values in the presence of f'' perturbations might be found in Eq. (26) for the shape of the output beam, which is completely determined by the values of only two constants, ϕ and γ, for given wavelength λ and distance R_0. (To simplify the discussion, we ignore the z^2 and slit convolution terms.) We previously used the exit beam only to obtain a value for ϕ, which is θ_0. If, however, by curve fitting, both ϕ and γ were determined, then we could solve Eq. (8) directly for

$$\alpha=\tfrac{1}{2}(\theta_i^2-\phi^2+\gamma^2) \tag{39}$$

or

$$f'=\frac{C}{2}(\theta_i^2-\phi^2+\gamma^2)-Z_T\ . \tag{40}$$

This approach would entail only a single measurement, with automatic correction for exactly the right value of f''. Estimates of ϕ and γ obtained from Fig. 3 of FWL suggest that γ will typically be 10—15 % of ϕ and, therefore, a small correction term after the squares are taken. We estimate that, for typical values for ϕ and γ, to obtain f' accuracy of $0.1e^-$ will require about 0.1% accuracy in both θ_i and ϕ. The γ^2 correction term only exceeds $0.1e^-$ for γ greater than about 2.0×10^{-4} (i.e., above the Ga edge). It is negligible for γ values less than 1.0×10^{-4}, meaning that the unexplained differences between computed and observed curve widths (see Sec. II B) seen for smaller γ values will not be significant. Whether ϕ and γ can indeed be extracted by curve fitting routines from real data with sufficient accuracy to make such an approach successful is a question which we shall address in another paper.

IV. CONCLUSIONS

The refraction of x-rays through a prism was analyzed in detail and expressions were derived both for the dependence of angle of refraction on absorption and for the profile of the refracted beam. The angle of refraction was found to include a term $\Delta f_a'$ which varies as the square of the anomalous scattering factor f'' and as the inverse square of the real angle of emergence θ_0. This correction term can become significant above absorption edges and when the incidence angle is close to the critical angle, making θ_0 small. The effect is small for the Ga data of FWL, being only about $\frac{1}{8}e^-$ above the Ga K edge, but was substantial above the As edge, approaching $1e^-$. The remaining inexplicable discrepancies between prism f' values and KK transformed EXAFS f' values are now comparable at both Ga and As edges and are presumed to arise from some as yet unidentified absorption mechanism.

The x-ray beam refracted by the prism was found to have a Cauchy profile described by two parameters, ϕ and γ, the real and imaginary parts of the complex sine of the emergent beam angle. Recognizing that f' may be evaluated directly from ϕ and γ, we suggested a technique for extracting f' values from curve fits to measured beam

profiles. If implementable, it would avoid those difficulties in making the $\Delta f_a'$ correction which arise from the need for an accurate knowledge of f''.

ACKNOWLEDGMENTS

The experimental data were obtained at Stanford Synchrotron Radiation Laboratory (SSRL), which is supported by the U.S. Department of Energy (Basic Energy Sciences Program and by the National Institutes of Health (Biotechnology Resource Program). One of us (W.K.W.) is supported by U.S. Department of Energy Contract No. DE-AM03-76SF00113 and by EG&G, Santa Barbara Operations, under Purchase Order No. 03-85EV72031.001. The other (K.F.L.) is supported by SSRL.

[1]A. Fontaine, W. K. Warburton, and K. F. Ludwig, Jr., Phys. Rev. B **31**, 3599 (1985).

[2]J. J. Hoyt, D. deFontaine, and W. K. Warburton, J. Appl. Crystallogr. **17**, 344 (1984).

[3]D. T. Cromer and D. Liberman, J. Chem. Phys. **53**, 1891 (1970).

[4]J. H. Underwood and T. W. Barbee, Jr., in *Low Energy X-ray Diagnostics, Monterey, California, 1981,* Proceedings of the Topical Conference on Low Energy X-ray Diagnostics, edited by D. T. Attwood and B. L. Henke (AIP, New York, 1981), pp. 170—178.

[5]J. A. Stratton, *Electromagnetic Theory* (McGraw-Hill, New York, 1941), pp. 500—504.

[6]M. Born and E. Wolf, *Principles of Optics,* 6th ed. (Pergamon, New York, 1983), pp. 615—617.

[7]J. A. Stratton, *Electromagnetic Theory,* Ref. 5, pp. 424—427.

[8]*Handbook of Mathematical Functions,* edited by M. Abramowitz and I. A. Stegun (Dover, New York, 1965), p. 71.

[9]C. Derman, L. J. Gleser, and I. Olkin, *A Guide to Probability Theory and Application* (Holt, Rinehart, and Winston, New York, 1973), pp. 414—418.

[10]R. W. James, *The Optical Principles of the Diffraction of X-rays* (Ox Bow, Woodbridge, CT, 1982), pp. 137—138.